Japanese Journal of Applied Physics

REGULAR PAPER

Evaluation of electron traps in SiN_x by discharge current transient spectroscopy: verification of validity by comparing with conventional DLTS

To cite this article: Harumi Seki *et al* 2019 *Jpn. J. Appl. Phys.* **58** SBBK02

Japanese Journal of Applied Physics **58**, SBBK02 (2019) **REGULAR PAPER**
https://doi.org/10.7567/1347-4065/aafe64

Evaluation of electron traps in SiN_x by discharge current transient spectroscopy: verification of validity by comparing with conventional DLTS

Harumi Seki*, Kazuhiko Yamamoto, and Yuichiro Mitani

Device Technology R&D Center, Institute of Memory Technology R&D, Toshiba Memory Corporation, Kawasaki, Kanagawa 212-8582, Japan

*E-mail: harumi.seki@toshiba.co.jp

Received September 28, 2018; revised November 19, 2018; accepted January 10, 2019; published online February 22, 2019

Discharge current transient spectroscopy (DCTS) is a promising technique for detecting the trap level and density in dielectrics because it is based on a simple emission process. In order to confirm the validity of DCTS, we compare the results from the conventional deep-level transient spectroscopy (DLTS) technique for samples of CVD-grown silicon nitride (SiN_x) films. Results indicated that a trap level, about 0.6 eV below the energy level of the conduction band edge in the SiN_x thin films estimated by DCTS is in good agreement with that obtained from DLTS analysis, and it is found that the trap density increases with the decreasing N/Si ratio in the SiN_x film. As a proposed estimation for energy level in defects, it will be originated from hydrogen-incorporated defects in the SiN_x matrix. This study demonstrates that the DCTS method will be a useful electrical method for the evaluation of defects.

1. Introduction

Silicon nitride (SiN_x) thin films have been widely used as a charge-trapping layer in metal/oxide/nitride/oxide/silicon (MONOS) memory.[1–3] The retention characteristics are affected by the energy level of the traps and its density.[4–6] The investigation of the physical properties of electron traps in SiN_x film is indispensable to improve the characteristics in charge-trap memory devices. Discharge current transient spectroscopy (DCTS) is proposed as one of the electrical evaluation methods for trap property.[7–10] Traps in an insulator can be investigated in terms of emission rate. The measurement setup and sequence of this technique are very simple. This is considered a powerful technique for evaluating the density and energy level of traps in an insulator. We have evaluated the electron traps in the SiN_x thin films.[11] However, there are relatively few reports on this method compared to reports about other evaluation techniques. In this paper, the trap level and its density in the SiN_x film are estimated by DCTS and conventional deep-level transient spectroscopy (DLTS).[12–20] DLTS is one of the well-known methods for determining the density and energy level of traps. DCTS and DLTS are similar methods where the observation is the transient response caused by electron emission from traps, but the response is detected as current and capacitance in DCTS and DLTS, respectively. We discuss the validity of the DCTS technique for the evaluation of electron traps by comparing the trap energy level with that obtained by DLTS[21] and also investigate more from the viewpoint of trap density.

2. Experimental methods

Metal-insulator-semiconductor (MIS) capacitors were used for both DCTS and DLTS measurements. SiN_x films on Si substrates were formed by CVD with SiH_2Cl_2 and NH_3, where different N/Si ratios were controlled by the gas flow rate. The physical thickness and composition of the SiN_x films were measured by transmission electron microscopy (TEM) and Rutherford backscattering spectroscopy (RBS), respectively, as listed in Table I.

Figure 1 shows the schematic diagram of the experimental setup with the cross-sectional view of an MIS capacitor (P-type Si substrate/SiN_x/P-doped poly-Si electrode) for DCTS. The MIS capacitor was charged by applying a positive voltage of 2.5 V to the substrate for 60 s. After the charge step, the voltage was set to zero, followed by the measurement of the discharge current through the poly-Si gate electrode. The sampling time was 100 ms during the first 10 s for the precise measurement of abrupt transient current, but after 10 s, it was set to 1 s to exclude the effect of noise from the measurement system. Measurement was performed in the temperature range from 238–278 K. DLTS measurement was carried out for the N-type Si substrate/SiN_x/Pd electrode stack capacitors in the constant-capacitance mode, as described in detail in the literature.[22,23] A positive voltage of 1.0 V was applied to the Pd electrode for 200 ms, and electrons were captured at trap sites in the SiN_x thin films. After charge, the transient voltage corresponding to the depletion layer width variation induced by the capture and emission of electrons was measured under constant capacitance of about 100 pF. The capacitance at threshold voltages determined as −0.53 to −0.55 V in the C–V curves (Fig. 2) were set as the measurement condition of the constant-capacitance DLTS. The temperature dependence of the transient voltage was measured in a range from 80–300 K.

Table I. Physical thickness and SiN_x composition (N/Si) measured by TEM and RBS.

Sample	Physical thickness (nm)	Composition (N/Si ratio)
A	10.6	1.23
B	10.9	1.11
C	11.5	1.05

3. Results and discussion

Trap levels and their density in SiN_x films can be estimated by the discharge current measurement in DCTS. When the dissipation of trapped charges in dielectrics obeys thermal emission from the traps to the conduction band, the discharge current $I_{dis}(t)$ is expressed as:

$$I_{dis}(t) = dQ(t)/dt = qSN_t De_n \exp(-e_n t), \quad (1)$$

where e_n is the emission rate from the traps to the conduction band of the SiN_x film, N_t is the trap density, S is the area of the electrode and D is the thickness of the SiN_x film. The

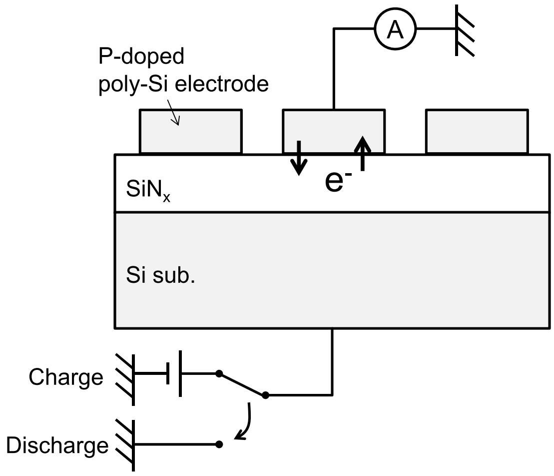

Fig. 1. Schematic diagram of the DCTS measurement setup for the MIS capacitor with SiN_x films. Electrons are injected by applying a positive substrate bias of 2.5 V for 60 s.

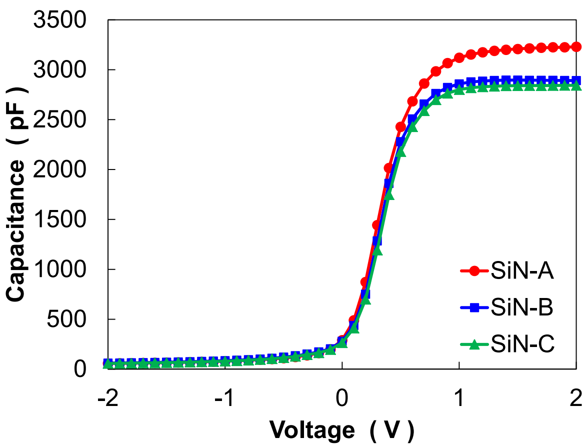

Fig. 2. (Color online) *C–V* characteristics of the MIS capacitor with SiN_x films. For constant-capacitance DLTS measurements, a capacitance of 100 pF was adjusted at the threshold voltage of around −0.54 V.

emission rate can be expressed as:

$$e_n = \nu \exp(-(E_c - E_t)/k_B T), \tag{2}$$

where E_c is the energy level of the conduction band edge, E_t is the trap energy level, ν is the attempt-to-escape frequency and T is the absolute temperature. From Eqs. (1) and (2), the following equations are obtained.

$$\ln I_{dis}(t) = \ln(qSN_t De_n) - e_n t, \tag{3}$$

$$\ln e_n = \ln \nu - (E_c - E_t)/k_B T. \tag{4}$$

By Eq. (4), the energy level of the traps (E_c-E_t) is deduced from e_n with its temperature dependence. The emission rate e_n can be obtained experimentally by fitting the discharge current using Eq. (1).

Figure 3 shows the discharge current with time as a function of measurement temperatures and nitrogen content in the SiN_x films. Solid lines are plotted as exponential curve fitting. The difference in time range of three samples is observed at each temperature. This difference suggests the variation in emission rates of these samples. Figure 4 shows the Arrhenius plot of the emission rate deduced from Fig. 3. Transient time becomes long with lower temperatures, corresponding to lower e_n due to stabilized electrons in the traps. Nitrogen concentration also affects the discharge current, possibly due to the different trap energy levels and their density as well. From the slope of the Arrhenius plot in Fig. 4 and with Eq. (4), the trap energy levels for samples A, B and C are estimated to be 0.64, 0.62 and 0.56 eV, respectively. It is found that Si-rich SiN_x film (sample C) has a shallower energy level with a higher emission rate than that of nitrogen-rich SiN_x. Here, we compare the results from the DCTS and DLTS measurements. Figure 5 shows typical DLTS spectra for SiN_x films with different nitrogen concentration where the deposition conditions were the same as those for DCTS. It is noteworthy that at least two discrete peaks, labeled T1 and T2, are observed for all samples. From the slopes of T1 and T2 on the Arrhenius plot (Fig. 6), the energy levels of traps for samples A, B and C were estimated to be 0.38, 0.42 and 0.43 eV for T1, and 0.60, 0.57 and 0.54 eV for T2, respectively. The energy levels of the electron traps deduced by DCTS and DLTS are summarized in Table II.

Figure 7 shows the composition dependence of trap levels with comparison for both DCTS and DLTS. The trap energy level estimated by DCTS is close to the value obtained from T2 peak in the DLTS spectrum. The shallower level observed as T1 peak in DLTS was not detected in the DCTS measurement. As shown in Fig. 5, T1 and T2 peaks were observed around 200 and 260 K, respectively. Since the measurement temperature region for DCTS (from 238–278 K) is consistent with T2 peak temperature, no detection for a shallower level is probably due to the high temperature during the DCTS measurement. For detailed analysis in DCTS, a measurement at a lower temperature is required. In the case of both DCTS and DLTS, the trap levels become shallower with a decrease in the N/Si ratio. A Poole–Frenkel trap study for different SiN_x composition has reported that the trap energy level decreases from 1.08 to 0.52 eV with a N/Si decrease from 1.33 to 0.54 (i.e. from Si_3N_4 to Si-rich SiN_x),[24,25] which is in good agreement with our study.

The trap density N_t estimated using Eq. (1) by DCTS increases with a decrease in the N/Si ratio, as shown in Fig. 8. For DLTS, the trap density is calculated under assumption of the existence of a trap site in the Si substrate. Although the absolute trap density estimation from DLTS measurement is impossible, we performed the qualitative consideration such as the composition dependence of trap density, as shown in Fig. 9. It is found that the trap density increases with Si content in SiN_x films, which is the same tendency for both DCTS and DLTS. We measured the Si–H bond density in the SiN_x films by Fourier transform infrared spectroscopy (data not shown). The increased trap density estimated by DCTS corresponds well to an increase in Si–H bond density, which is shown in a previous report.[10] The composition dependence of the trap density in DCTS and DLTS measurement might be caused by the difference in Si–H bond density in SiN_x film. Since the trap level and the composition dependence of the trap density established by DCTS shows agreement with that obtained by T2 peak in the DLTS spectrum, it is considered that DCTS and DLTS measurements seem to detect the same traps in the SiN_x thin films.

The incorporation of hydrogen atoms into nitrogen vacancies and the effect on the electron trap level were analyzed by

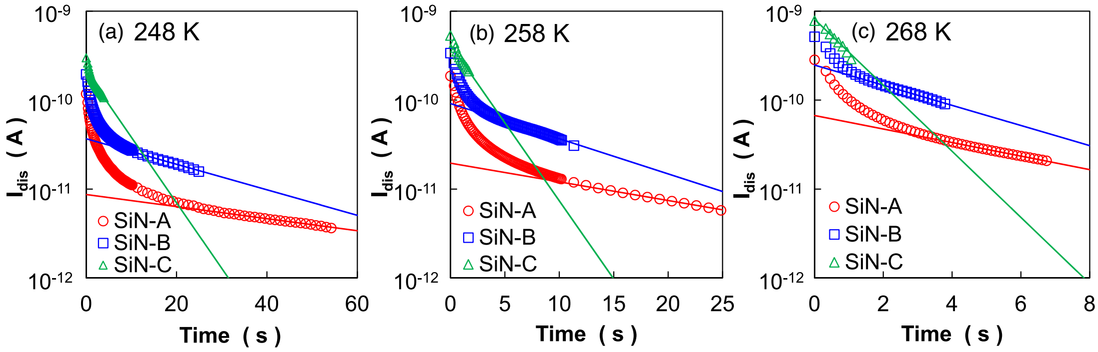

Fig. 3. (Color online) Composition dependence of discharge current measured at various temperatures. Solid lines show exponential approximation fitting.

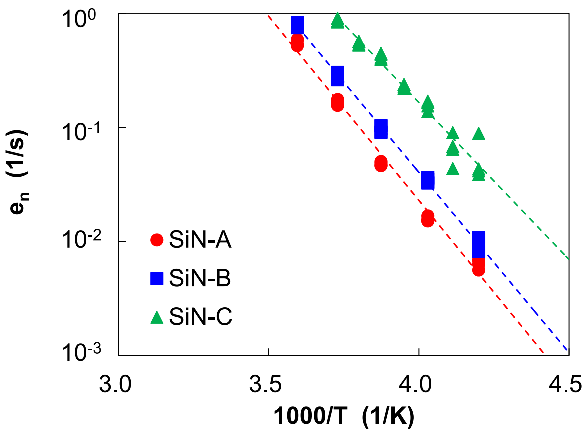

Fig. 4. (Color online) Arrhenius plot of emission rate (e_n) as a function of nitrogen content in the SiN_x films.

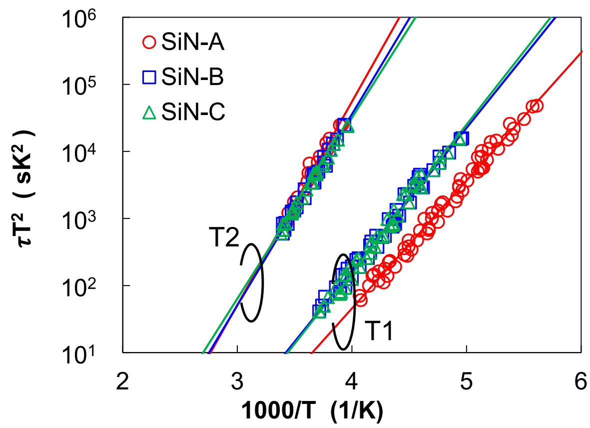

Fig. 6. (Color online) Arrhenius plot of τT^2 as a function of the nitrogen content in the SiN_x films. Slope corresponds to the electron trap level (E_c-E_t).

simulation for Si_3N_4 (N/Si = 1.33).[26–30] The trap levels caused by nitrogen vacancy (above 2.0 eV) become shallower by hydrogen incorporation, and split on the H-site position to be 0.9 and 0.6 eV.[26] Since two trap levels below 0.9 eV are obtained in this study, it is inferred that DCTS and DLTS measurements detect the hydrogen-incorporated defects in SiN_x films. The trap energy levels of about 0.6 and 0.4 eV established by our experiment are shallower than the simulated trap energy levels. As mentioned above, trap level shallowing with a decrease in the N/Si ratio is reported. The N/Si ratio of 1.05–1.25 for samples A, B and C are lower than that of Si_3N_4 in the simulation study. The difference between the energy levels of the traps analyzed by simulation and those evaluated by DCTS and DLTS is considered to be caused by the difference in SiN_x composition.

Table II. Energy level of electron trap evaluated by DCTS and DLTS. Trap energy level estimated by DCTS shows agreement with that obtained from T2 peak of DLTS spectrum.

Sample	Energy level of electron trap (eV)		
	DCTS (240–280 K)	DLTS	
		T1 (∼200 K)	T2 (∼260 K)
A	0.64	0.38	0.60
B	0.62	0.42	0.57
C	0.56	0.43	0.54

The deep trap level caused by nitrogen vacancy is not detected under our DCTS experimental conditions. To improve the characteristics in MONOS memory, the investigation of deep traps as well as shallow traps is important.

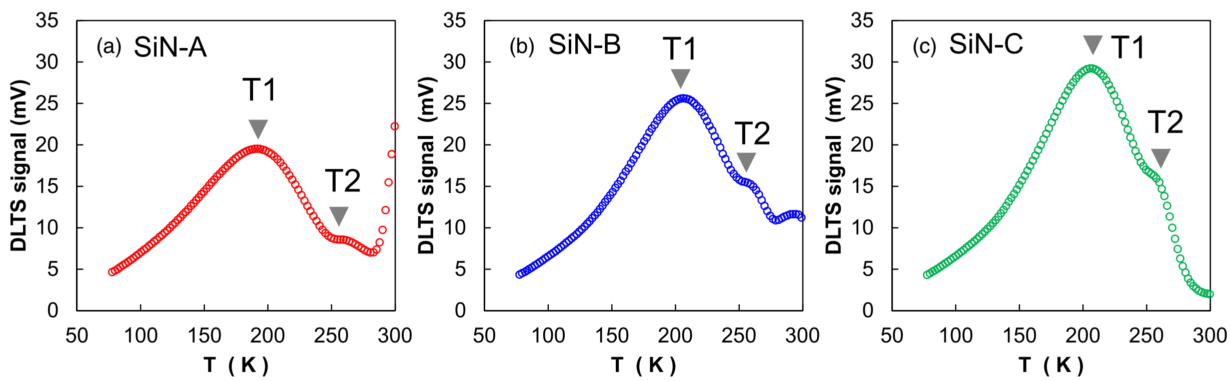

Fig. 5. (Color online) Composition dependence of DLTS spectra. Two peaks of T1 and T2 for lower and higher were detected, respectively.

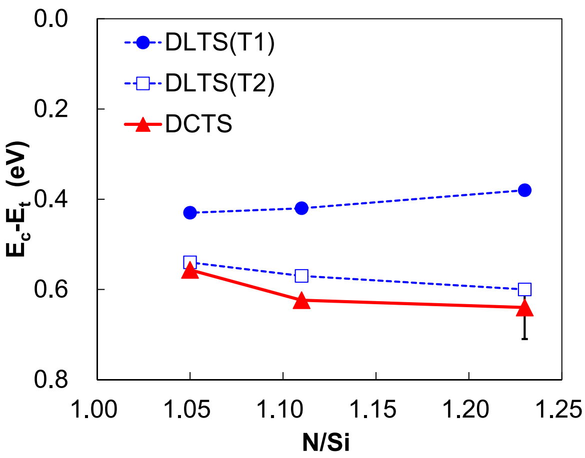

Fig. 7. (Color online) Composition dependence of trap energy levels deduced by DCTS and DLTS. Trap energy level estimated by DCTS shows good agreement with that obtained by T2 peak in the DLTS spectrum.

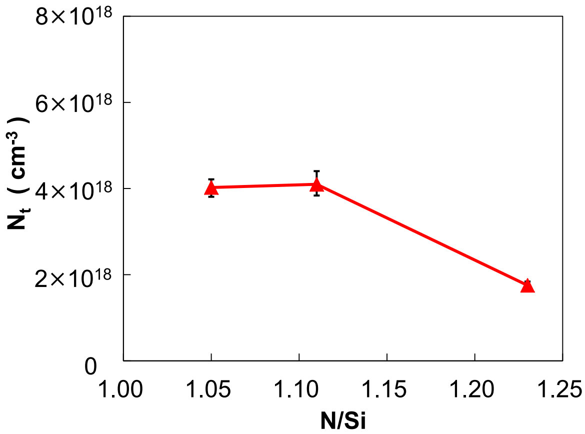

Fig. 8. (Color online) Composition dependence of the trap density estimated by DCTS. Trap density shows an increase with a decrease in the N/Si ratio.

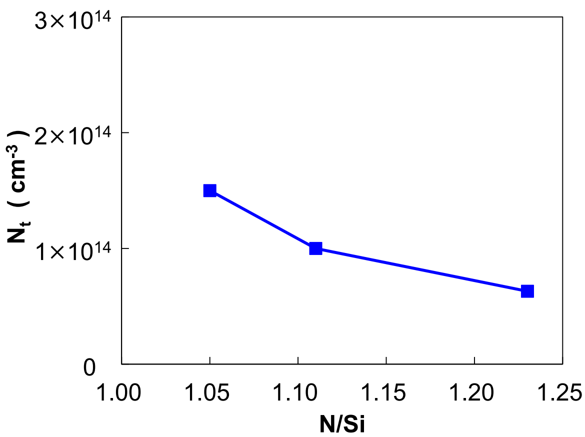

Fig. 9. (Color online) Composition dependence of the trap density estimated by T2 peak in the DLTS spectrum. Absolute trap density estimation is impossible because the calculation is performed under assumption of the existence of a trap site in the Si substrate.

Improving the minimum detection sensitivity of the discharge current and raising the emission probability by high-temperature measurement is required for the evaluation of deeper-level traps by DCTS.

4. Conclusions

The energy levels of the electron traps and their density were measured by DCTS and DLTS. In both methods, the trap energy levels around 0.6 eV are obtained and become shallower with a decrease in the N/Si ratio. The trap density obtained by DCTS and DLTS increases with a decrease in the N/Si ratio. Since the trap energy level and its density obtained by DCTS show agreement with those from DLTS, it can be concluded that DCTS and DLTS evaluated the same trap in the SiN_x thin films. The validity of the DCTS method is confirmed by comparison of the trap energy levels and their density with those evaluated by the well-known DLTS method. The traps detected by DCTS and DLTS are considered to be caused by hydrogen-incorporated defects.

1) S. Minami and Y. Kamigaki, IEEE Trans. Electron Devices **40**, 2011 (1993).
2) S. Fujii, R. Fujitsuka, K. Sekine, M. Koyama, and N. Yasuda, Jpn. J. Appl. Phys. **51**, 124302 (2012).
3) Y. Ren, K. J. Weber, N. M. Nursam, and D. Wang, Appl. Phys. Lett. **97**, 202907 (2010).
4) T. H. Kim, J. S. Sim, J. D. Lee, H. C. Shin, and B.-G. Park, Appl. Phys. Lett. **85**, 660 (2004).
5) E. Vianello, F. Driusi, A. Arreghini, P. Palestri, D. Esseni, L. Selmi, N. Akil, M. J. Duuren, and D. S. Golubovic, IEEE Trans. Electron Devices **56**, 1980 (2009).
6) S. Fujii, H. Kusai, K. Sakuma, and M. Koyama, Jpn. J. Appl. Phys. **53**, 058005 (2014).
7) H. Matsuura, M. Yoshimoto, and H. Matsunami, Jpn. J. Appl. Phys. **34**, L185 (1995).
8) H. Matsuura, M. Yoshimoto, and H. Matsunami, Jpn. J. Appl. Phys. **34**, L371 (1995).
9) H. Aozasa, I. Fujiwara, A. Nakamura, and Y. Komatsu, Jpn. J. Appl. Phys. **38**, 1441 (1999).
10) H. Aozasa, I. Fujiwara, and Y. Kamigaki, Jpn. J. Appl. Phys. **46**, 5762 (2007).
11) H. Seki, Y. Kamimuta, and Y. Mitani, Jpn. J. Appl. Phys. **57**, 06KB04 (2018).
12) D. V. Lang, J. Appl. Phys. **45**, 3023 (1974).
13) Y. Yamashita, T. Sato, M. E. Bayu, K. Toko, and T. Suemasu, Jpn. J. Appl. Phys. **57**, 075801 (2018).
14) H. Wakimoto, H. Nakazawa, T. Matsumoto, and Y. Nabetani, J. Appl. Phys. **123**, 161422 (2018).
15) C. Gong, E. Simoen, N. Posthuma, E. V. Kerschaver, J. Poortmans, and R. Mertens, Appl. Phys. Lett. **96**, 103507 (2010).
16) J. Schmidt and A. G. Aberle, J. Appl. Phys. **85**, 3626 (1999).
17) A. Ricksand and O. Engstrom, J. Appl. Phys. **70**, 6915 (1991).
18) J. C. Simpson and J. F. Cardaro, J. Appl. Phys. **63**, 1781 (1988).
19) W. Gotz, N. M. Johnson, H. Amano, and I. Akasaki, Appl. Phys. Lett. **65**, 463 (1994).
20) Y. S. Yang, S. H. Kim, J.-I. Lee, H. Y. Chu, L.-M. Do, H. Lee, J. Oh, T. Zyung, M. K. Ryu, and M. S. Jang, Appl. Phys. Lett. **80**, 1595 (2002).
21) H. Seki and Y. Mitani, Ext. Abstr. Int. Conf. Solid State Devices and Materials. 2018, p. 325.
22) N. M. Johnson, J. Vac. Sci. Technol. **21**, 303 (1982).
23) N. M. Johnson, D. J. Bartelink, R. B. Gold, and J. F. Gibbons, J. Appl. Phys. **50**, 4828 (1979).
24) S. Habermehl and C. Carmignani, Appl. Phys. Lett. **80**, 261 (2002).
25) S. Habermehl and R. T. Apodaca, Appl. Phys. Lett. **84**, 215 (2004).
26) K. Sonoda, E. Tsukuda, M. Tanizawa, and Y. Yamaguchi, J. Appl. Phys. **117**, 104501 (2015).
27) K. Yamaguchi, A. Otake, K. Kamiya, Y. Shigeta, and K. Shiraishi, Jpn. J. Appl. Phys. **50**, 04DD05 (2011).
28) K. Kamiya, K. Yamaguchi, A. Otake, Y. Shigeta, and K. Shiraishi, ECS Trans. **41**, 71 (2011).
29) K. Yamaguchi, A. Otake, K. Kamiya, K. Shigeta, and Y. Shigeta, Int. Conf. Simulation on Semiconductor Process and Devices, 2011, p. 215.
30) A. Otake, K. Yamaguchi, K. Kamiya, Y. Shigeta, and K. Shiraishi, IEICE Trans. Electron. **E94**, 693 (2011).